

# Magnetic Electrochemical Sensing Platform for Biomonitoring of Exposure to Organophosphorus Pesticides and Nerve Agents Based on Simultaneous Measurement of Total Enzyme Amount and Enzyme Activity

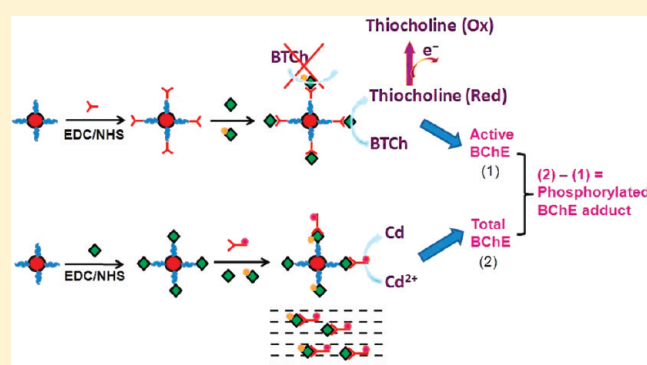
Dan Du,<sup>†,‡</sup> Jun Wang,<sup>\*,‡</sup> Limin Wang,<sup>‡</sup> Donglai Lu,<sup>‡</sup> Jordan N. Smith,<sup>‡</sup> Charles Timchalk,<sup>‡</sup> and Yuehe Lin<sup>\*,‡</sup>

<sup>†</sup>Key Laboratory of Pesticide and Chemical Biology of Ministry of Education, College of Chemistry, Central China Normal University, Wuhan 430079, People's Republic of China

<sup>‡</sup>Pacific Northwest National Laboratory, Richland, Washington 99352, United States

**S** Supporting Information

**ABSTRACT:** We report a new approach for electrochemical quantification of enzymatic inhibition and phosphorylation for biomonitoring of exposure to organophosphorus (OP) pesticides and nerve agents based on a magnetic bead (MB) immunosensing platform. The principle of this approach is based on the combination of MB immunocapture-based enzyme activity assay and competitive immunoassay of the total amount of enzyme for simultaneous detection of enzyme inhibition and phosphorylation in biological fluids. Butyrylcholinesterase (BChE) was chosen as a model enzyme. In competitive immunoassay, the target BChE in a sample competes with the BChE immobilized on the MBs to bind to the limited sites of anti-BChE antibody labeled with quantum dots (QD–anti-BChE), followed by stripping voltammetric analysis of the bound QD conjugate on the MBs. This assay shows a linear response over the total BChE concentration range of 0.1–20 nM. Simultaneous real time BChE activity was measured on an electrochemical carbon nanotube-based sensor coupled with a microflow injection system after immunocapture by the MB–anti-BChE conjugate. Therefore, the formed phosphorylated BChE adduct (OP–BChE) can be estimated by the difference values of the total amount of BChE (including active and OP-inhibited) and active BChE from established calibration curves. This approach not only eliminates the difficulty in screening of low-dose OP exposure (less than 20% inhibition of BChE) because of individual variation of BChE values but also avoids the drawback of the scarce availability of OP–BChE antibody. It is sensitive enough to detect 0.5 nM OP–BChE, which is less than 2% BChE inhibition. This method offers a new method for rapid, accurate, selective, and inexpensive quantification of OP–BChE and enzyme inhibition for biomonitoring of OP and nerve agent exposures.



With an increased risk and threat to people's health resulting from the ongoing use of organophosphorus (OP) compounds, such as pesticides and potential exposure to chemical nerve agents in terrorist attacks, in military activities, or from accidents, there is a need to develop new and improved countermeasures for such events.<sup>1,2</sup> Development of more effective diagnostic technologies for rapid detection of these exposures is essential. A simple, portable, durable, and reliable diagnosis tool is needed for biological monitoring, to screen poison victims for the initiation of appropriate medical treatments, and to effectively triage nonexposed individuals during a mass casualty event.

Following exposure, OP pesticides and nerve agents readily interact with enzymes and proteins within the biological matrix to produce a number of relevant biomarkers, including the following: (i) OP adducts by phosphorylation of proteins, including enzymes, resulting in the loss of enzyme (e.g., cholinesterase) activity; (ii) metabolites by hydrolysis; (iii) unbound free OP

in fluids.<sup>3</sup> All are typical biomarkers of exposure to OP agents; therefore, some methods such as enzyme activity assays,<sup>4</sup> immunoassays of OP adducts<sup>5–7</sup> and metabolites, and GC/LC MS analysis of OP adducts, metabolites, and free OPs have been developed for biomonitoring of exposure to OP agents.<sup>8,9</sup> However, for simple and rapid diagnosis/screening, especially in emergency cases, laboratory-based analytical methods (GC/LC MS) are not ideal because of lack of portability and lack of real time results.<sup>10,11</sup> Immunoassays of OP adducts or metabolites for diagnosis of OP exposure are challenged because of unavailability of OP-specific antibodies. Hence, the most utilized detection method is to measure enzyme activity, since it is a rapid and simple method for OP exposure evaluation and risk

**Received:** January 29, 2011

**Accepted:** April 4, 2011

**Published:** April 04, 2011

assessment.<sup>12,13</sup> Some methods, including the colorimetric Ellman assay,<sup>14</sup> fluorescence assays,<sup>15</sup> the Michel ( $\Delta$ pH) ChE assay,<sup>16</sup> radioactive assays,<sup>17</sup> and the Walter Reed Army Institute of Research (WRAIR) assay,<sup>18,19</sup> have been developed. However, these methods require a baseline or a control for an individual in order to detect meaningful changes in blood enzyme levels.<sup>20</sup> Generally, a statistically derived value of enzyme activity from a large amount of people serves as this baseline. These methods are not accurate and may provide ambiguous results at subclinical exposure (less than 20% enzyme inhibition) because of inter- and intraindividual variations (e.g., sex, age, ethnicity, etc.) in the normal levels of BChE between individuals.<sup>4</sup> To help address this issue, we have developed a method based on reactivation of phosphorylated ChE to evaluate OP exposure. This method shows some advantages, such as baseline-free, sensitive, and accurate, but it is not useful for some OP exposures in which the phosphorylated enzymes can either spontaneously regenerate or quickly age (irreversibly inhibited).<sup>21</sup> Moreover, none of these enzyme activity-based methods provide any quantitative information for the formed OP adducts. In this regard, novel methods for simple, rapid, accurate, and reliable detection/screening of exposure to OP agents are highly desirable.

Thus far, little attention has been paid to combining the enzyme activity assay with an immunoassay for detecting/screening OP exposures. Herein, we propose a novel approach for simple and rapid detection of exposure to OP agents on the basis of the combination of immunocapture-based enzyme activity assay and immunoassay of the total amount of enzyme simultaneously for detection of enzyme inhibition and phosphorylation in biological fluids, both of which are typical biomarkers of OP exposure. This approach is based on a hypothesis that the catalytic capability of cholinesterase is the same between individuals, and the key to the method is that the quantitative dependence of enzyme activity on its concentration could be established prior to OP exposures. Therefore, the measured enzyme activity from a postexposure directly indicates active enzyme levels in a given sample, and the total amount of enzyme (including active and inhibited) detected serves as a control. As such, it is easy to quantify both enzyme inhibition and phosphorylation from postexposure samples, providing a convenient way for screening/assessing exposure to OP agents.

In this paper, we report on a novel sensing platform based on magnetic immunodetection for simultaneously measuring enzyme activity and the total amount of enzyme for diagnosis/screening exposure to OP agents. To achieve specificity of the method, butyrylcholinesterase (BChE) antibodies immobilized on magnetic beads (MBs) are used to capture BChE in samples and detect enzyme activity. Simultaneously, MB-based competitive immunoassay of the total amount of enzyme is performed using electrochemical techniques. The difference values of the total amount of BChE and active BChE derived from an established calibration curve of enzyme vs concentration are used to estimate the formed OP–BChE adduct in the serum. We chose BChE as a model analyte to demonstrate the principle-of-concept of this method because BChE reacts quickly with OP at low concentrations and the symptoms of acute toxicity always correlate with inhibition of BChE.<sup>4</sup> In addition, BChE is abundant in human plasma, allowing for sensitive detection required for low-level exposure. Here, MBs were used as a sensing platform because of its inherent advantages such as good stability, versatility

in chemical modification, and ease of separation.<sup>22–24</sup> This approach not only eliminates the difficulty in screening of low-dose OP exposures of less than 20% inhibition of BChE but also avoids the drawback of the unavailability of OP-specific antibodies for quantifying phosphorylated adduct. This method is baseline-free, and it offers a new avenue for rapid, accurate, selective, and inexpensive biomonitoring of a variety of OP exposures.

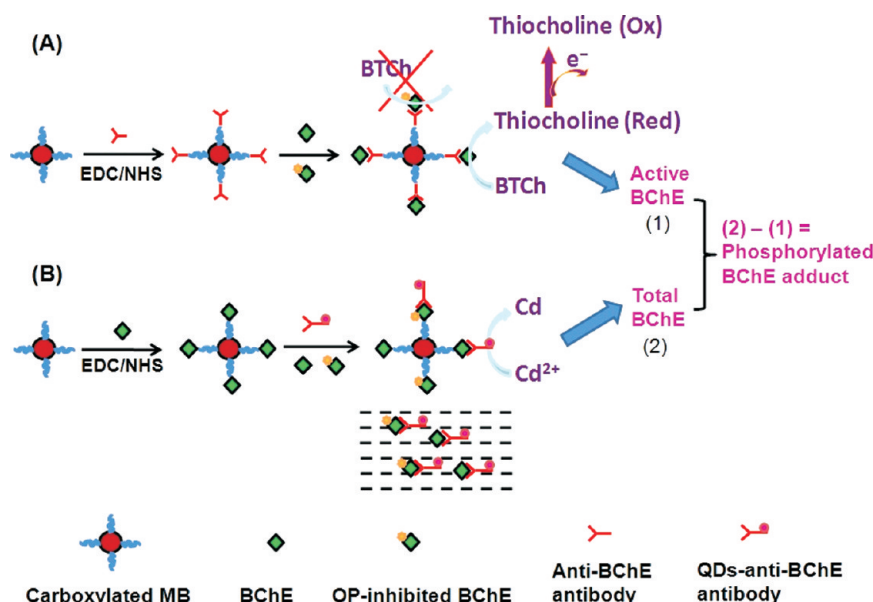
## ■ EXPERIMENTAL SECTION

**Reagents.** Qdot@625 antibody conjugation kit, which was purchased from Molecular Probes Inc. (Eugene, OR), includes QDs (CdS@ZnS), succinimidyl *trans*-4-(*N*-maleimidylmethyl)-cyclohexane-1-carboxylate solution, dithiothreitol (DDT) solution, dye-labeled marker for antibody elution, mercaptoethanol, separation media, and exchange buffer. Human BChE, butyrylthiocholine (BTCh), bovine serum albumin (BSA), Tween-20, 1-ethyl-3-(3-dimethylaminopropyl)carbodiimide hydrochloride (EDC), *N*-hydroxysuccinimide (NHS), 3,3',5,5'-tetramethylbenzidine (TMB), phosphate-buffered saline (PBS), and 2-(*N*-morpholino)ethanesulfonic acid (MES) were products from Sigma-Aldrich Co. (St. Louis, MO). Anti-BChE antibody (ab17246) was purchased from Abcam Inc. (Cambridge, MA). Carboxyl-functionalized MBs (20 mg/mL,  $5 \times 10^8$  MBs/mg) were obtained from Polysciences, Inc. (Warrington, PA). SuperBlock T20 (TBS) blocking buffer and bicinchoninic acid assay (BCA) kit were purchased from Thermo Scientific (Rockford, IL). Paraoxon was purchased from Chem Service, Inc. (West Chester, PA). Microplates for enzyme-linked immunosorbent assay (ELISA) were purchased from Becton (Franklin Lakes, NJ). All stock and buffer solutions were prepared using autoclaved double-deionized water. Mixed human plasma with sodium heparin as the anticoagulant was procured from Biorclamation Inc. (Liverpool, NY).

**Apparatus.** All electrochemical measurements were performed with an electrochemical analyzer CHI 824 (CH Instruments, Austin, TX) connected to a personal computer. For square wave voltammetry (SWV) measurement, the disposable screen printed carbon electrode (SPCE) or multiwalled carbon nanotube electrode (110CNT) consisting of a carbon working electrode, a carbon counter electrode, and an Ag/AgCl reference electrode was purchased from Dropsens, Inc. (Spain) for electrochemical measurements. A sensor connector (Dropsens, Inc.) allows for connection of the SPCE to the CHI electrochemical analyzer. Magnetic capturing and separations were conducted on an MCB 1200 Biomagnetic Processing Platform (Sigris, CA). ELISA measurements were carried out at room temperature on a Safire 2 microplate reader (TECAN, Switzerland). A transmission electron microscope (TEM, Hitachi H-7000) was used to characterize sample suspensions, each of which was dropped onto carbonate film-coated copper grids (3-mm diameter, 200 mesh) to be dried at room temperature and then measured at 75 kV. X-ray photoelectron spectroscopy (XPS) measurements were taken with a Physical Electronics Quantum 2000 Scanning Microprobe.

**Conjugation of anti-BChE Antibody and BChE with MBs.** The conjugation of anti-BChE antibody and BChE with MBs was processed by EDC/NHS chemistry (see Supporting Information). From UV results, an average number of  $\sim 1.1 \times 10^5$  anti-BChE antibodies per MB or 20 nM MB–anti-BChE conjugate were obtained (see Supporting Information).

**Scheme 1. Schematic Illustrations of the Principle of Immunosensing Platform Based on (A) Immunodetection of Enzyme Activity and (B) Immunoassay of Total Amount of Enzyme Simultaneously for Biomonitoring of OP Exposure**



MB–anti-BChE and MB–BChE conjugates are stable at 4 °C for at least 4 weeks.

**Preparation of QD–anti-BChE Antibody Conjugates.** QD–anti-BChE antibody conjugates were prepared by following the protocol for the Qdot@625 antibody conjugation kit (see Supporting Information).

**Preparation of Phosphorylated BChE Adduct and Human Plasma Samples.** Phosphorylated adduct was prepared by the incubation of BChE or human plasma samples with paraoxon as a model of OPs (see Supporting Information).

**Testing of Immunoaffinity of anti-BChE Antibody to BChE and OP–BChE by ELISA.** The immunoaffinity of anti-BChE antibody to BChE and OP–BChE was examined by ELISA (see Supporting Information).

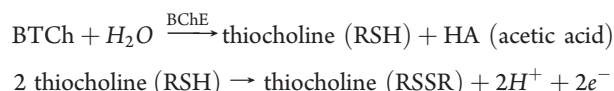
**Competitive Immunoassays of the Total Amount of BChE.** Competitive immunoassays of the total amount of BChE using electrochemical SWV measurement include three steps: (1) competitive capturing of BChE in samples or plasma samples; (2) releasing the QD label captured on the surface of MBs; (3) electrochemical SWV detection (see Supporting Information).

**Electrochemical Immunosensing of Active BChE.** Electrochemical quantification of the active BChE using flow injection sensing system includes two steps: (1) magnetic capturing of BChE from samples; (2) electrochemical detection of enzyme activity with the flow injection system (see Supporting Information).

## RESULTS AND DISCUSSION

**MB Immunosensing Platform for Quantification of Exposure to OP Agents.** Scheme 1 illustrates the principle of combination of enzyme activity assay and immunoassay for detecting OP exposures. Briefly, one sensor detects enzyme activity using MB–anti-BChE conjugates to capture BChE in the samples (mixture of OP-inhibited BChE and active BChE) followed by electrochemical detection of electroactive enzymatic

products thiocholine (A) based on the reactions:



As such, enzyme activity measured from samples can be used to calculate active enzyme according to an established calibration curve of enzyme activity vs enzyme concentration. Here, multi-wall carbon nanotubes (MWCNTs) are used to enhance the signal from oxidation of enzymatic products. Simultaneously, the other sensor can detect total enzyme (mixture of OP-inhibited BChE and active BChE) based on competitive immunoassay using MB–BChE conjugates (B). In this platform, BChE was conjugated to MBs, and QDs served as a label for enhancing signal output. In the assay, the target BChE (mixture of OP-inhibited BChE and active BChE) in samples competes with BChE conjugated on the MBs to bind to the limited binding sites of the QD–anti-BChE conjugate in the incubation solution. Upon completion of the immunoreaction, electrochemical measurements were used to quantify the total amount of BChE by analysis of cadmium ions released from captured quantum dots. Both the total real time enzyme amount and the enzyme activity can be detected in the sample; therefore, we can achieve both enzyme inhibition and the phosphorylation adduct in samples for detection of exposure to OP agents.

**TEM Characterization of MBs and MB Conjugates.** Figure 1 illustrates typical TEM images of negatively stained samples including carboxylated MBs (A), MB–BChE/QD–anti-BChE conjugate (B), and QD–anti-BChE (C). Magnified images are shown in panels D and E. Carboxylated MB shows an average size of  $\sim 1 \mu\text{m}$  with a smooth surface (Figure 1A). Also individual QD–anti-BChE conjugates are clearly identifiable and appear uniform in size with a diameter of 10 nm (Figure 1C). When BChE were first covalently linked to carboxylated MB and then followed by competitive immunoreactions between MB–BChE



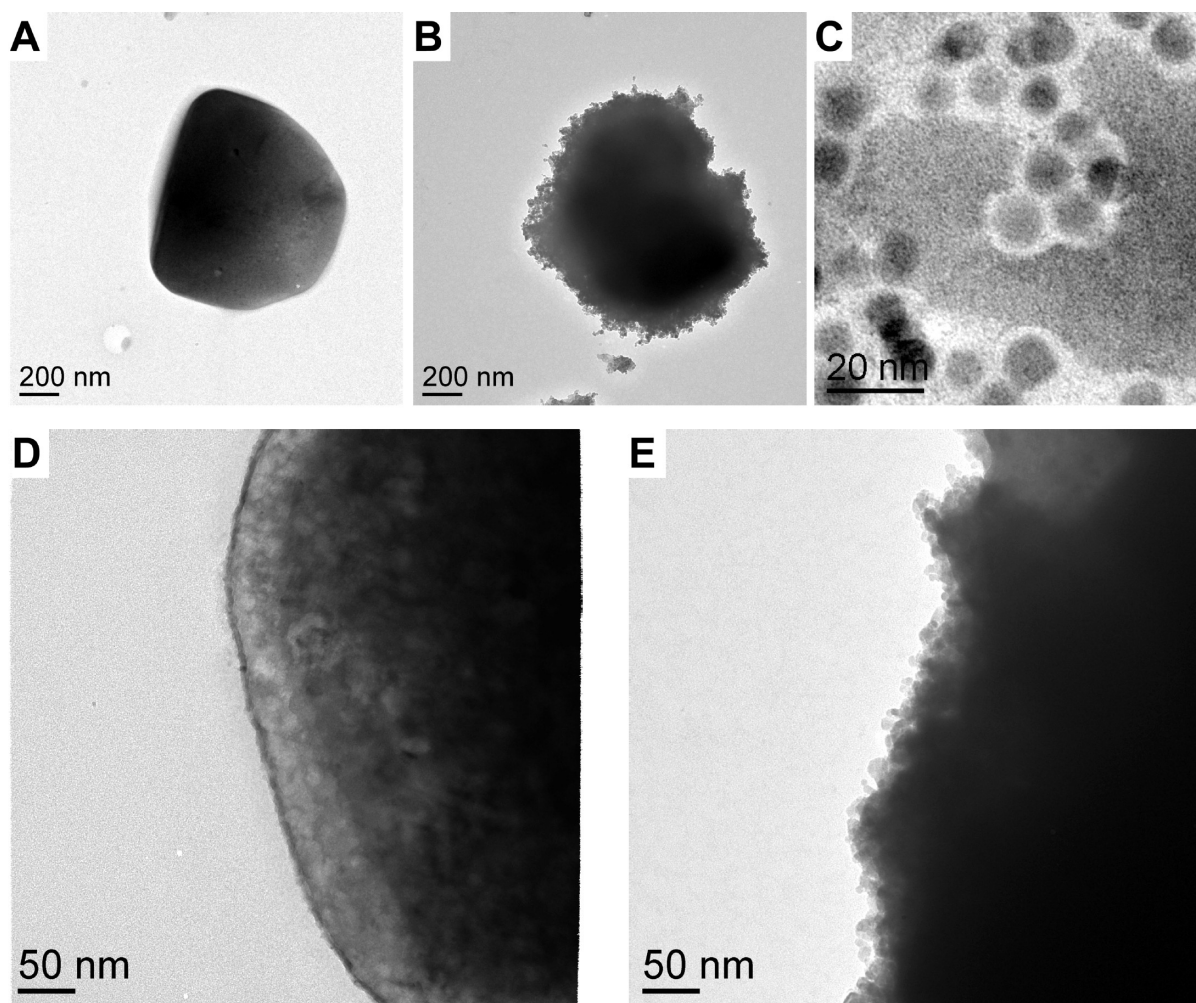


**Figure 1.** Typical TEM images of (A) carboxylated MBs, (B) MB-BChE/QD-anti-BChE conjugates, (C) QD-anti-BChE. (D) Magnified image of carboxylated MBs and (E) magnified image of MB-BChE/QD-anti-BChE.

and QD-anti-BChE, the formed MB-BChE/QD-anti-BChE immunocomplex results in an increase of surface roughness of the MBs (Figure 1B). Detailed magnified images of carboxylated MBs (Figure 1D) and MB-BChE/QD-anti-BChE (Figure 1E) further display smooth and rough lateral surfaces, respectively.

**XPS Analysis of Carboxyl-Functionalized MBs and MB Conjugates.** XPS spectra of the carboxyl-functionalized MBs (curve a), MB-anti-BChE conjugate (curve b), and MB-BChE conjugate (curve c) are shown in Figure S1 in Supporting Information. All MBs showed the binding energy of the core electrons for the  $C_{1s}$  line at 285.0 eV from the C-H groups (Figure S1A). The carboxyl-functionalized MBs were confirmed by the obvious signal in the peak at 288.1 eV (curve a), which was attributed to the COOH unit.<sup>25</sup> After MB binding with BChE or anti-BChE antibody, the peak of COOH shifted slightly left and appeared at 287.6 eV (curves b and c in Figure S1B), which might be attributed to the interaction between EDC/NHS-activated carboxylate of MBs and amino groups on the antibody or antigen. Furthermore, a strong  $N_{1s}$  binding energy at 399.6 eV was observed in the MB-anti-BChE conjugate (curve b) and MB-BChE conjugate (curve c) as shown in Figure S1B, while a much smaller signal could be detected on the MBs (curve a) which comes from surface polymer containing N. The  $N_{1s}$  core level spectra showed a typical binding energy of the amide nitrogen

atoms ( $HN-C=O$ ) coming from the function of antibodies and antigens,<sup>26</sup> indicating successful modification of MBs with BChE or anti-BChE.

**Electrochemical Characterization of BChE Activity Based on MB-anti-BChE Capturing.** As shown above, active BChE can hydrolyze its substrate BTCh to produce thiocholine which is electroactive and detectable at the CNT/SPCE by application of a low potential. The CNT is used to decrease the overpotential and enhance the electrochemical signal because of its high surface area, excellent electrical conductivity, and electrocatalytic activity.<sup>27–29</sup> The activity of BChE was inhibited with paraoxon, resulting in a phosphorylated OP-BChE adduct and decrease electrochemical signals. The BChE activity was studied by cyclic voltammetry using the proposed method. As shown in Figure 2A, after incubation of MB-anti-BChE with 10 nM BChE, the formed MB-anti-BChE/BChE immunocomplex displayed no detectable redox peaks on the bare SPCE (curve a) and CNT/SPCE (curve b) in PBS buffer (pH 7.4) because no substrates were present. However, when BTCh was added into the PBS, an obvious oxidation peak was observed on both bare SPCE (curve c) and CNT/SPCE (curve d) at 780 mV and 583 mV, respectively. Since no peaks were observed for the BTCh solution on both electrodes (data not shown), the peak is obviously attributed to the oxidation of thiocholine, the hydrolysis product of BTCh

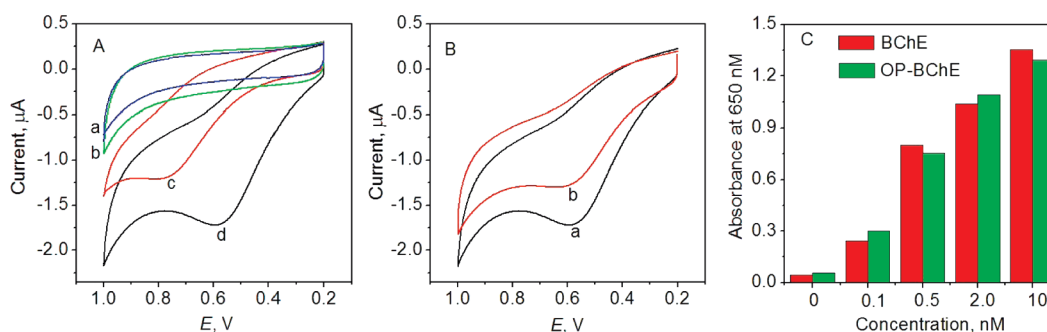


**Figure 2.** (A) Cyclic voltammograms obtained at MB–anti-BChE/BChE immunocomplex coated on (a) bare SPCE and (b) CNT/SPCE in PBS, and on (c) bare SPCE and (d) CNTs/SPCE in PBS containing 5 mM BTCh. (B) Cyclic voltammograms obtained at the MB–anti-BChE/BChE immunocomplex coated on CNT/SPCE in PBS containing 5 mM BTCh after incubating MB–anti-BChE (a) with 10 nM BChE and (b) with 5 nM BChE and 5 nM paraoxon–BChE mixture for 40 min. (C) ELISA assay of anti-BChE antibody for recognition of (red) BChE and (green) OP–BChE.

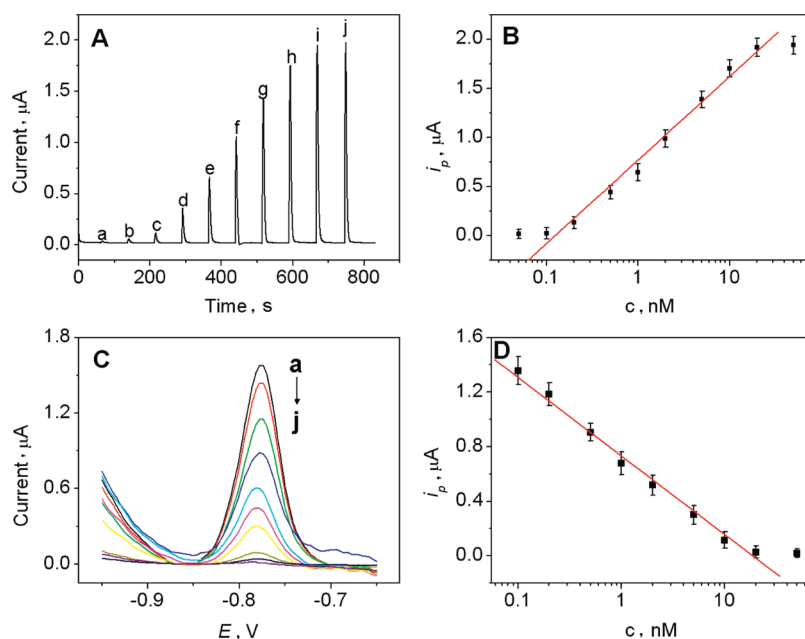


**Figure 3.** (A) Amperometric responses for MB–anti-BChE incubated with different concentrations of BChE: (a) 0.05 nM; (b) 0.1 nM; (c) 0.2 nM; (d) 0.5 nM; (e) 1.0 nM; (f) 2.0 nM; (g) 5.0 nM; (h) 10 nM; (i) 20 nM; (j) 50 nM. (B) Calibration plot for BChE activity and concentration. (C) SWV responses for MB–BChE incubated with different concentrations of BChE: (a) 0 nM; (b) 0.1 nM; (c) 0.2 nM; (d) 0.5 nM; (e) 1.0 nM; (f) 2.0 nM; (g) 5.0 nM; (h) 10 nM; (i) 20 nM; (j) 50 nM. (D) Calibration plot for SWV response and BChE concentration.

which was catalyzed by the active BChE on the MB–anti-BChE/BChE immunoconjugate. Furthermore, the oxidation peak current on the CNT/SPCE was much higher than that on the bare SPCE and the peak potential shifted negatively  $\sim 200$  mV. These results revealed that CNTs can greatly enhance the electrochemical signal of the enzymatic product and decrease the overpotential of thiocholine oxidation. The decrease of the overpotential is beneficial for avoiding interferences from other electroactive species in biological matrices. Here, cyclic voltammetric measurements were further used to understand the effects of OP exposure on the BChE activity as shown in Figure 2B. When 5 nM BChE and 5 nM paraoxon–BChE mixture solution was incubated with MB–anti-BChE, the peak current of the immunoconjugate on the CNTs/SPCE decreased greatly (curve b) compared to that of 10 nM BChE incubation (curve a). It is evident that paraoxon inhibits BChE enzyme activity, resulting in the decreased electrochemical response. These results also

demonstrate that the immunocapture electrochemical detection approach is capable of measuring the enzyme activity in samples.

Furthermore, we studied the immunoaffinities of anti-BChE antibody to both BChE and OP–BChE by ELISA (Figure 2C). Almost equal absorbance values were observed for anti-BChE antibodies recognizing both BChE and OP–BChE at the same concentrations, demonstrating that anti-BChE can equally recognize both BChE and OP–BChE. It is very important to confirm the equal binding affinity of anti-BChE antibodies to BChE and OP–BChE because we want to use an immunoassay to measure the total amount of BChE including active BChE and OP-inhibited BChE from samples exposed to OPs. The same affinity of anti-BChE to both BChE and OP–BChE is critical to this method. Otherwise, this method cannot be used to measure the total amount of BChE. Furthermore, only when anti-BChE equally recognizes both BChE and OP–BChE can we conclude that the decrease of peak current at the sensor for

Table 1. Comparison of Calculated and Known OP–BChE in Artificially Prepared BChE Samples

	sample no.					
	1	2	3	4	5	6
added BChE ( $c_1$ , nM)	10	9.5	8	4	1	0
added OP–BChE ( $c_2$ , nM)	0	0.5	2	6	9	10
total added BChE + OP–BChE ( $c_0$ , nM)	10	10	10	10	10	10
determined total BChE + OP–BChE from immunoreaction curve ( $c_0'$ , nM)	10.19	9.67	10.05	10.13	9.64	9.71
determined BChE from activity curve ( $c_1'$ , nM)	10.15	9.21	7.89	3.72	1.12	0.09
determined OP–BChE ( $c_2' = c_0' - c_1'$ , nM)	0.04	0.46	2.16	6.41	8.52	9.62
relative deviations ( $(c_2' - c_2)/c_2 \times 100\%$ )	—	−8.0%	+8.0%	+6.8%	−5.3%	−3.8%
determined phosphorylation percent ( $P\% = (c_2'/c_0') \times 100\%$ )	0.39%	4.76%	21.50%	63.28%	88.38%	99.07%

immunoenzyme activity assay stems from the resulting phosphorylated adducts, rather than immunoaffinities.

**Optimization of Assays.** To improve the sensitivity of electrochemical detection of enzyme activity and total BChE by the immunocapture approach, we optimized the MB concentration (A), incubation time for immunoreactions (B), BTCh reaction time (C), and volume of QD–anti-BChE (D), and the results are shown in Figure S2 in Supporting Information.

**Establishment of a Quantitative Relationship between Enzyme Activity and Enzyme Concentration.** To explore the quantitative relationship between enzyme activity and concentration, we used purified human serum BChE as a standard. In this study, MB–anti-BChE was first incubated with different concentrations of standard BChE for 40 min, and the formed MB–anti-BChE/BChE immunocomplex was then reacted with BTCh for 5 min. After magnetic separation, the final reaction solution was collected and injected into the flow injection sensing system for amperometric measurements (Figure 3A). It can be seen that the electrochemical signals increase with an increase of BChE concentrations. A linear response is obtained over the concentration range from 0.1 nM to 20 nM, with the regression equation of  $i_p$  ( $\mu\text{A}$ ) = 0.7716 + 0.8497lgc (nM) (1) and the correlation coefficient of 0.9935 (Figure 3B). The detection limit is calculated to be as low as 0.05 nM.

**Competitive Immunoassay of the Total Amount of BChE.** Under optimal conditions, a competitive immunoassay configuration was used for the determination of the total target amount of BChE. Figure 3C shows the SWV responses of different concentrations of BChE at a SPCE. The target BChE at a known concentration competes with captured BChE on the MBs to bind to the limited binding sites of the QD–anti-BChE conjugate in the incubation solution. As expected for a competitive mechanism, the SWV peak current from the captured QDs on the MB–BChE shows a decrease with an increase of target BChE concentrations in the incubation solution. The resulting calibration curve is linear between SWV responses and BChE concentrations over the range of 0.1–20 nM, with the regression equation of  $i_p$  ( $\mu\text{A}$ ) = 0.7331 − 0.5753lgc (nM) (2) and the correlation coefficient of 0.9956 (Figure 3D). The detection limit is calculated to be 0.05 nM.

**Performance of the Sensing Platform for Measurement of Phosphorylated Adducts and Enzyme Inhibition.** To demonstrate the capability of the sensing platform for quantification of phosphorylated adducts by simultaneous detection of enzyme activity and total amount of BChE, we used simulated samples containing different concentrations of standard BChE and OP–BChE. Briefly, these samples were prepared by mixing a

series of standard BChE of known concentrations with phosphorylated adducts of OP–BChE at different ratios (Table 1). Each sample was measured using the proposed sensing platform for detecting enzyme activity and total BChE, and all the results are shown in Table 1. Measured OP–BChE concentrations are consistent with the added known OP–BChE values for all the samples, and the relative deviations are lower than 8.0%, indicating that this new quantitative approach is applicable and reliable for OP–BChE analysis. Since the average concentration of BChE in serum is 40–70 nM,<sup>30–32</sup> this method is sensitive enough to detect 0.5 nM OP–BChE, which is less than 2% BChE inhibition. Furthermore, the percentage of phosphorylated BChE in these samples could be obtained by this method (Table 1), which is consistent with the values from the prepared samples, indicating that this method is accurate and reliable.

**Validation of the Sensing Platform with Paraoxon-Dosed Human Plasma Samples.** The validation of the sensing platform for biomonitoring OP exposure was further explored with in vitro paraoxon-dosed human plasma samples. A series of human plasma samples was prepared by incubating with various concentrations of paraoxon. First, enzyme activity of these samples was detected by the proposed sensing platform. As shown in Figure S3A, the plasma sample control displayed the maximum current (peak a) and the amperometric signal decreased with increasing paraoxon concentrations (peaks b, c, d, e, f, g, h, and i). The observed amperometric signal inversely correlates with paraoxon concentration, indicating that a decrease in enzymatic activity was directly related to phosphorylation of enzymes by OP exposure. Since BChE reacts quickly with OP at low concentrations, the symptoms of acute toxicity always correlate with the inhibition of BChE.

In parallel, the total amount of BChE for each sample was determined by competitive immunoassay according to calibration curve 2. Therefore, the amount of OP–BChE adduct formed in the plasma could be estimated by subtracting the active BChE concentration obtained from the calibration curve 1. These results were listed in Table S1 in Supporting Information. The relationship between OP–BChE adduct and OP concentration in human samples was further plotted (Figure S3B). Table S1 and Figure S3B show that the formed OP–BChE adducts increase with increasing concentration of paraoxon at low doses. However, the increase in phosphorylation slows down at high dose (>180 nM). The percentage of phosphorylation in these samples was also calculated (Table S1). We found that the maximum value of % phosphorylation of BChE in the sample is about 96% even at high dose of exposure to paraoxon, indicating



that some phosphorylated BChE may be reversible. This reversibility was likely attributed to the binding equilibrium between pesticide and binding sites in enzyme. This is first time we have used phosphorylation data to explain why the enzyme inhibition obtained by Ellman assay is always less than 100% even at high doses. We further calculated total enzyme activity via the calibration curve (1) for each sample assumed prior to the OP exposure. Thus, enzyme inhibition for each sample could be measured. A plot of enzyme inhibition vs OP concentration was obtained (curve a in Figure S3C), which was consistent with the curve obtained by Ellman assay (curve b in Figure S3C).

## CONCLUSIONS

We have developed a novel immunocapture/electrochemical detection platform for the biomonitoring of exposure to OP agents based on simultaneous immunodetection of enzyme activity and immunoassay of the total amount of enzyme in the samples. The novelty of this method relies on the following: (1) the use of antibody to selectively capture enzyme for the enzyme activity assay, overcoming the lack of specificity of the conventional Ellman assay; (2) combination of the immunocapture for enzyme activity assay and immunoassay of total enzyme for the biomonitoring of exposure to OP agents. Such a method offers great advantages: (i) baseline-free; (ii) good selectivity; (iii) good sensitivity (less than 2% BChE inhibition); (iv) no need for OP-specific antibody quantitation of phosphorylated enzyme; (v) less interference because magnetic beads are used for separation of analytes from biological matrixes; (vi) simple, portable, and inexpensive. Overall, the proposed method has a great potential for realizing an accurate, sensitive, rapid, and low-cost onsite biomonitoring of OP exposure and diagnosis/screening of victims after OP exposures.

## ASSOCIATED CONTENT

**S Supporting Information.** Additional information as noted in the text. This material is available free of charge via the Internet at <http://pubs.acs.org>.

## AUTHOR INFORMATION

### Corresponding Author

\*E-mail: [jun.wang@pnl.gov](mailto:jun.wang@pnl.gov) (J.W.); [yuehe.lin@pnl.gov](mailto:yuehe.lin@pnl.gov) (Y.L.).

## ACKNOWLEDGMENT

The work was performed at Pacific Northwest National Laboratory (PNNL) and supported partially by grant number U01 NS058161-01 from the National Institutes of Health CounterACT Program through the National Institute of Neurological Disorders and Stroke, NIH, and CDC/NIOSH Grant R01 OH008173-01. This work was also supported partially by the National Natural Science Foundation of China (21075047), the Program for Chenguang Young Scientist for Wuhan (200950431184), and the Special Fund for Basic Scientific Research of Central Colleges (CCNU10A02005). A portion of the research was performed using EMSL, a national scientific user facility sponsored by the Department of Energy's Office of Biological and Environmental Research and located at Pacific Northwest National Laboratory. PNNL is operated by Battelle for DOE under Contract DE-AC05-76RL01830. The authors

thank Alice Dohnalkova for the TEM experiment and Mark H. Engelhard for the XPS analysis.

## REFERENCES

- (1) Quinn, D. M. *Chem. Rev.* **1987**, *87*, 955–979.
- (2) Tu, A. T. *Toxin Rev.* **2007**, *26*, 231–274.
- (3) Liu, G. D.; Wang, J.; Barry, R.; Petersen, C.; Timchalk, C.; Gassman, P. L.; Lin, Y. H. *Chem.—Eur. J.* **2008**, *14*, 9951–9959.
- (4) Lockridge, O.; Schopfer, L. M.; Masson, P. In *Handbook of Toxicology of Chemical Warfare Agents*; Gupta, R. C., Ed.; Academic Press: New York, 2009; Chapter 56, pp 847–858.
- (5) Wang, H.; Wang, J.; Timchalk, C.; Lin, Y. H. *Anal. Chem.* **2008**, *80*, 8477–8484.
- (6) Khattab, A. D.; Ali, I. S. *Environ. Toxicol. Pharmacol.* **2007**, *24*, 275–285.
- (7) Sporty, J. L. S.; Lemire, S. W.; Jakubowski, E. M.; Renner, J. A.; Evans, R. A.; Williams, R. F.; Schmidt, J. G.; van der Schans, M. J.; Noort, D.; Johnson, R. C. *Anal. Chem.* **2010**, *82*, 6593–6600.
- (8) Holland, K. E.; Solano, M. I.; Johnson, R. C.; Maggio, V. L.; Barr, J. R. *J. Anal. Toxicol.* **2008**, *32*, 116–124.
- (9) Li, H.; Ricordel, I.; Tong, L.; Schopfer, L. M.; Baud, F.; Megarbane, B.; Maury, E.; Masson, P.; Lockridge, O. *J. Appl. Toxicol.* **2009**, *29*, 149–155.
- (10) Adams, T. K.; Capacio, B. R.; Smith, J. R.; Whalley, C. E.; Korte, W. D. *Drug Chem. Toxicol.* **2004**, *27*, 77–91.
- (11) Noort, D.; Fidler, A.; van der Schans, M. J.; Hulst, A. G. *Anal. Chem.* **2006**, *78*, 6640–6644.
- (12) Wang, J.; Timchalk, C.; Lin, Y. H. *Environ. Sci. Technol.* **2008**, *42*, 2688–2693.
- (13) Black, R. M.; Noort, D. In *Chemical Warfare Agents: Toxicology and Treatment*; Marrs, T. C.; Maynard, R. L.; Sidell, F. R., Eds.; John Wiley & Sons Ltd: New York, 2007; Chapter 5, pp 127–156.
- (14) Ellman, G. L.; Courtney, K. D.; Andres, V., Jr.; Feather-Stone, R. M. *Biochem. Pharmacol.* **1961**, *7*, 88–95.
- (15) Parvari, R.; Pecht, I.; Soreq, H. *Anal. Biochem.* **1983**, *133*, 450–456.
- (16) Ellin, R. I.; Burkhardt, B. H.; Hart, R. D. *Arch. Environ. Health* **1973**, *27*, 48–49.
- (17) Gordon, R. K.; Doctor, B. P.; Chiang, P. K. *Anal. Biochem.* **1982**, *124*, 333–337.
- (18) Gordon, R. K.; Haigh, J. R.; Garcia, G. E.; Feaster, S. R.; Riel, M. A.; Lenz, D. E.; Aisen, P. S.; Doctor, B. P. *Chem. Biol. Interact.* **2005**, *157–158*, 239–246.
- (19) Haigh, J. R.; Lefkowitz, L. J.; Capacio, B. R.; Doctor, B. P.; Gordon, R. K. *Chem. Biol. Interact.* **2008**, *175*, 417–420.
- (20) Jun, D.; Bajgar, J.; Kuca, K.; Kassa, J. In *Handbook of Toxicology of Chemical Warfare Agents*; Gupta, R. C., Ed.; Academic Press: New York, 2009; Chapter 58, pp 877–886.
- (21) Du, D.; Wang, J.; Smith, J. N.; Timchalk, C.; Lin, Y. H. *Anal. Chem.* **2009**, *81*, 9314–9320.
- (22) Acharya, G.; Chang, C. L.; Doorneweerd, D. D.; Vlashi, E.; Henne, W. A.; Hartmann, L. C.; Low, P. S.; Savran, C. A. *J. Am. Chem. Soc.* **2007**, *129*, 15824–15829.
- (23) Mani, V.; Chikkaveeraiah, B. V.; Patel, V.; Silvio Gutkind, J.; Rusling, J. F. *ACS Nano* **2009**, *3*, 585–594.
- (24) Kim, B. C.; Ju, M. K.; Yu-Dan-Chin, A.; Sommer, P. *Anal. Chem.* **2009**, *81*, 2388–2393.
- (25) Shen, G.; Anand, M. F. G.; Levicky, R. *Nucleic Acids Res.* **2004**, *32*, 5973–5980.
- (26) Darain, F.; Gan, K. L.; Tjin, S. C. *Biomed. Microdevices* **2009**, *11*, 653–661.
- (27) Tasis, D.; Tagmatarchis, N.; Bianco, A.; Prato, M. *Chem. Rev.* **2006**, *106*, 1105–1136.
- (28) Yu, X.; Munge, B.; Patel, Y.; Jensen, G.; Bhirde, A.; Gong, J. D.; Kim, S. N.; Gillespie, J.; Gutkind, J. S.; Papadimitrakopoulos, F.; Rusling, J. F. *J. Am. Chem. Soc.* **2006**, *128*, 11199–11205.

- (29) Du, D.; Huang, X.; Cai, J.; Zhang, A. D.; Ding, J. W.; Chen, S. Z. *Anal. Bioanal. Chem.* **2007**, 387, 1059–1065.
- (30) Masson, P.; Lockridge, O. *Arch. Biochem. Biophys.* **2010**, 494, 107–120.
- (31) Bartels, C. F.; Xie, W.; Miller-Lindholm, A. K.; Schopfer, L. M.; Lockridge, O. *Biochem. Pharmacol.* **2000**, 60, 479–487.
- (32) Jun, D.; Bajgar, J.; Kuca, K.; Kassa, J. In *Handbook of Toxicology of Chemical Warfare Agents*; Gupta, R. C., Ed.; Academic Press: New York, 2009; Chapter 58, pp 877–886.